Hypertension Research (2017) 40, 117–129

www.nature.com/hr

ORIGINAL ARTICLE

Notch activation of Ca^{2+}-sensing receptor mediates hypoxia-induced pulmonary hypertension

Qiang Guo, Hua Xu, Xinjing Yang, Daguo Zhao, Shenlang Liu, Xue Sun and Jian-an Huang

A recent study from our group demonstrated that the Ca^{2+}-sensing receptor (CaSR) was upregulated and that the extracellular Ca^{2+}-induced increase in the cytosolic Ca^{2+} concentration $[Ca^{2+}]_{cyt}$ was enhanced in pulmonary arterial smooth muscle cells (PASMCs) from patients with idiopathic pulmonary arterial hypertension. Here, we examined whether hypoxia-induced activation of Notch signaling leads to the activation and upregulation of CaSR in hypoxia-induced pulmonary hypertension (HPH). The activation of Notch signaling with Jag-1, a Notch ligand, can activate the function and increase the expression of CaSR in acute and chronic hypoxic PASMCs. Downregulation of Notch3 with a siRNA attenuates the extracellular Ca^{2+}-induced increase in $[Ca^{2+}]_{cyt}$ and the increase in hypoxia-induced PASMC proliferation in acute hypoxic rat PASMCs. Furthermore, we tested the prevention and rescue effects of a γ-secretase inhibitor (DAPT) in HPH rats. For the Jag-1-treated group, right ventricular systolic pressure (RVSP), right heart hypertrophy (RV/LV+S ratio), and the level of right ventricular myocardial fibrosis were higher than the hypoxia alone group. Meanwhile, DAPT treatment prevented and rescued pulmonary hypertension in HPH rats. The Notch activation of CaSR mediates hypoxia-induced pulmonary hypertension. Understanding the new molecular mechanisms that regulate $[Ca^{2+}]_{cyt}$ and PASMC proliferation is critical to elucidating the pathogenesis of HPH and the development of novel therapies for pulmonary hypertension.
Hypertension Research (2017) **40,** 117–129; doi:10.1038/hr.2016.118; published online 1 September 2016

Keywords: hypoxia; Notch signaling; pulmonary hypertension; rat

INTRODUCTION

Pulmonary hypertension (PH) is characterized by a progressive increase in pulmonary vascular resistance and vascular remodeling, which, without treatment, leads to right heart failure and death, often within 2–3 years of diagnosis.[1–4] Hypoxia-induced pulmonary hypertension (HPH) occurs in patients with chronic obstructive pulmonary disease and obstructive sleep apnea and is a risk factor for right heart failure.[5,6] Currently, there are limited options available for the prevention and treatment of HPH. The pathogenesis of HPH can be attributed in part to excessive vascular remodeling, resulting in elevated pulmonary vascular resistance.[1,7,8] An increase in the cytosolic Ca^{2+} concentrations ($[Ca^{2+}]_{cyt}$) in pulmonary arterial smooth muscle cells (PASMCs) is an important stimulus for pulmonary vasoconstriction and vascular remodeling.

A recent study indicated that the extracellular Ca^{2+}-sensing receptor (CaSR) is involved in the enhanced Ca^{2+} influx and proliferation of pulmonary arterial smooth muscle cells (PASMCs) in patients with idiopathic pulmonary arterial hypertension.[9] $[Ca^{2+}]_{cyt}$ has an important role in the regulation of contraction, proliferation and migration of PASMCs. The elevation of $[Ca^{2+}]_{cyt}$ in PASMCs results from Ca^{2+} release from intracellular stores and Ca^{2+} influx through plasmalemmal Ca^{2+} channels.[1,10–15]

CaSR is a GPCR (belonging to Family C GPCRs) with 1085 amino acids.[16–18] CaSR senses the extracellular Ca^{2+} concentration and transduces it into the intracellular space through multiple signaling pathways.[16–22] CaSR also interacts directly with G proteins (Gqα and G11α). The activation of CaSR by extracellular Ca^{2+} (or calcimimetics) induces an increase in $[Ca^{2+}]_{cyt}$ through PLC-mediated hydrolysis of phosphatidylinositol-4,5- bisphosphate (PIP_2) to inositol-1,4, 5- trisphosphate (IP_3) and diacylglycerol. IP_3 binds to the IP_3 receptor (IP_3R) on the SR membrane and induces Ca^{2+} release from the SR to the cytosol.[16–21]

Notch signaling is involved in vascular development, and Notch3 has recently been implicated in pulmonary hypertension.[23,24] The lung tissue from patients with pulmonary hypertension displays increased Notch3 and Notch3 intracellular domain (N3ICD) expression compared with normotensive patients.[24] In addition, Notch3 and N3ICD expression are increased in two animal models of pulmonary hypertension, HPH in mice and monocrotoline-induced pulmonary hypertension in rats, and Notch knockout blocks the development of HPH in mice.[24] We have recently shown that activation of Notch signaling via treatment with the Notch ligand Jagged-1 (Jag-1) enhances store-operated Ca^{2+} entry in PASMCs.[25] Another recent study from our group demonstrates that hypoxia-induced activation of

Department of Medicine, Respiratory, Emergency and Critical Care Medicine, The First Affiliated Hospital of Soochow University, Suzhou, China
Correspondence: Professor Q Guo, Department of Medicine, Respiratory, Infectious, Emergency and Critical Care Medicine, The First Affiliated Hospital of Soochow University, 188 Shizhi Street, Suzhou 215006, China.
E-mail: ggqq1018@hotmail.com
Received 10 May 2016; revised 15 July 2016; accepted 25 July 2016; published online 1 September 2016

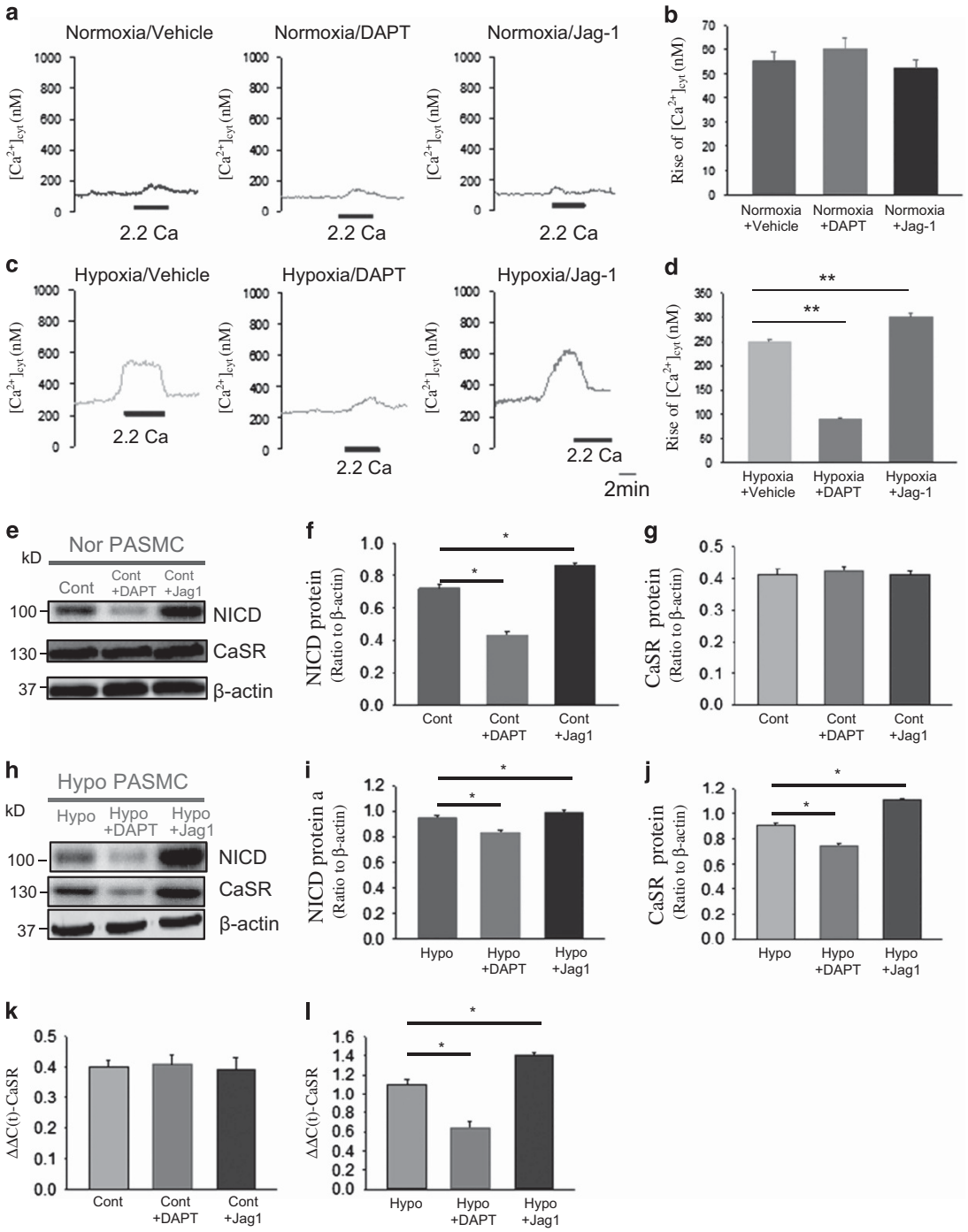

Figure 1 The extracellular Ca^{2+}-induced increase in $[Ca^{2+}]_{cyt}$ in acute hypoxic rat pulmonary arterial smooth muscle cells (PASMCs) was enhanced by Jag-1 and restored to normal levels by a γ-secretase inhibitor (DAPT). The Jag-1 treatment significantly enhanced the increased $[Ca^{2+}]_{cyt}$ in hypoxic PASMCs *in vitro*. The DAPT treatment significantly restored the increased $[Ca^{2+}]_{cyt}$ in hypoxic PASMCs *in vitro* (**c** and **d**). No differences were observed in the increased $[Ca^{2+}]_{cyt}$ between the normoxia+vehicle, normoxia+Jag-1 and normoxia+DAPT groups (**a** and **b**). Real-time PCR analyses of Ca^{2+}-sensing receptor (CaSR) expression in PASMCs 48 h after the DAPT or Jag-1 treatments. The expression of the CaSR messenger RNA (mRNA) was increased by Jag-1 and decreased by DAPT, but only in the hypoxic condition (**k** and **l**). The expression of the CaSR protein in the hypoxia+Jag-1 group was significantly increased compared with the hypoxia+vehicle group (**h** and **j**). The expression of the CaSR protein in the hypoxia+DAPT group was significantly decreased compared with the hypoxia+vehicle group (**h** and **j**). The expression of the Notch intracellular domain (NICD) protein was increased by Jag-1 and decreased by DAPT (**e**–**g** and **i**). No differences were observed between the normoxia+vehicle and normoxia+DAPT groups or between the normoxia+vehicle and normoxia+Jag-1 groups (**e**). A full color version of this figure is available at *Hypertension Research* online.

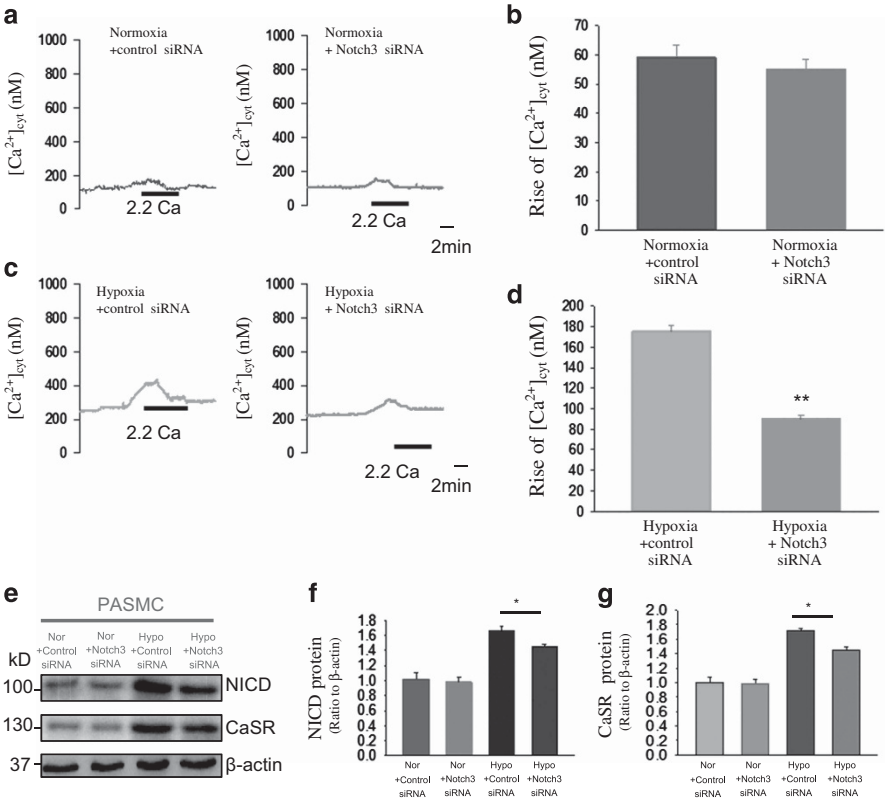

Figure 2 Downregulation of Notch3 with a small interfering RNA (siRNA) attenuates the extracellular Ca^{2+}-induced increase in $[Ca^{2+}]_{cyt}$ in acute hypoxic rat pulmonary arterial smooth muscle cells (PASMCs). (**a**) and (**b**) Representative records of the $[Ca^{2+}]_{cyt}$ changes and summarized data showing the extracellular Ca^{2+}-induced $[Ca^{2+}]_{cyt}$ increases in normoxic PASMCs transfected with the control-siRNA ($n=52$) and Notch3-siRNA ($n=53$). (**c**) and (**d**) Representative records of the $[Ca^{2+}]_{cyt}$ changes and summarized data showing the extracellular Ca^{2+}-induced $[Ca^{2+}]_{cyt}$ increases in acute hypoxic PASMCs transfected with control-siRNA ($n=55$) and Notch3-siRNA ($n=57$). $^{**}P<0.01$ *vs.* control-siRNA. (**e**–**g**) Western blot and analysis of the summarized data for Notch intracellular domain (NICD; **f**) and Ca^{2+}-sensing receptor (CaSR; **g**) in normoxic and hypoxic PASMCs treated with the control (or scrambled) siRNA (control) and Notch3-siRNA (at 25 and 50 nmol/l, $n=3$ per group). A full color version of this figure is available at *Hypertension Research* online.

Notch signaling mediates HPV and the development of HPH via the functional activation and upregulation of TRPC6 channels.[26]

In this study, we investigated the role of CaSR in the responses to changes in Notch signaling. Our results indicate that activation of Notch signaling increases the extracellular Ca^{2+}-induced increase in $[Ca^{2+}]_{cyt}$ in PASMCs in HPH. Finally, we show that Notch-mediated activation of the CaSR contributes to hypoxia-induced pulmonary hypertension.

MATERIALS AND METHODS

Preparation of animal PASMCs

The approval to use the animal lung tissues and cells was granted by Soochow University. In some experiments, we used freshly dissociated primary rat PASMCs.[27,28]

Cell culture and hypoxia

Rat PASMCs were cultured in Medium 199 supplemented with 10% fetal bovine serum (Life Technologies, Grand Island, NY, USA), 100 U ml^{-1} penicillin, 100 μg ml^{-1} streptomycin (Life Technologies), 50 μg ml^{-1} D-valine (Sigma-Aldrich, St Louis, MO, USA) and 20 μg ml^{-1} endothelial cell growth supplement (BD Biosciences, Franklin Lakes, NJ, USA) at 37 °C.[9] After reaching confluence, the cells were subcultured by trypsinization with 0.05% Trypsin-EDTA (Life Technologies). For the hypoxia experiments, PASMCs were cultured in an incubator with 3% O_2. For the DAPT- or Jag-1-treated groups, PASMCs were treated with DAPT (10 μM) or Jag-1 (50 μM) for 72 h.

$[Ca^{2+}]_{cyt}$ measurements

$[Ca^{2+}]_{cyt}$ was measured in PASMCs using fura-2 and a Nikon digital fluorescent imaging system.[8] The cells were loaded with 4 μmol l^{-1} fura-2 acetoxymethyl ester (fura-2/AM) for 60 min at 25 °C, and $[Ca^{2+}]_{cyt}$ was measured using a ratiometric method at 32 °C. PASMCs were superfused with a Ca^{2+}-free solution (plus 1 mmol l^{-1} EGTA for 10 min), and restoration of the extracellular Ca^{2+} levels (2.2 mmol l^{-1}) in the bath solution had no effect on $[Ca^{2+}]_{cyt}$.[9]

Preparation of HPH rats

All the experiments were approved by the Ethics/Animal Care Committee of Soochow University.

For the experiments with the HPH rats, male Sprague Dawley rats (190–200 g) were exposed to hypoxia (10% O_2) in a ventilated chamber to induce pulmonary hypertension. For the DAPT- or Jag-1-treated groups, the rats were intraperitoneally injected with DAPT (10.0 mg kg^{-1} per day from days 14 to 24) or Jag-1 (0.1 mg kg^{-1} per day from days 14 to 24) in the rescue experiments. The HPH rats were intraperitoneally injected with DAPT (10.0 mg kg^{-1} per day from days 1 to 14) or Jag-1 (0.1 mg kg^{-1} per day from days 1 to 14) in the prevention experiments. Four weeks after exposure to normobaric hypoxia, the rats were anesthetized with ketamine/xylazine, and right ventricular systolic pressure (RVSP) was then measured by right heart catheterization using an MPVS Ultra system (Millar Instruments, Suzhou, China).

Hemodynamic measurements

The animals were initially intraperitoneally anesthetized with ketamine (100 mg kg^{-1}) and xylazine (26 mg kg^{-1}). RVSP was determined with a

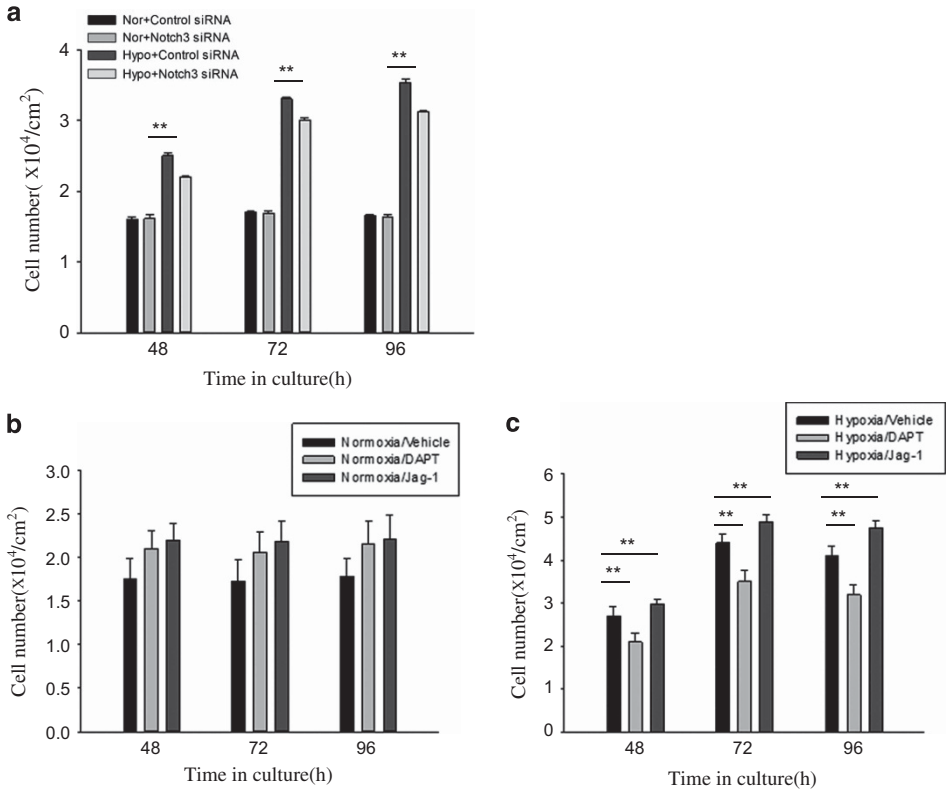

Figure 3 Downregulation of Notch3 with a small interfering RNA (siRNA) attenuates the increase in hypoxia-induced pulmonary arterial smooth muscle cell (PASMC) proliferation. The increase in hypoxia-induced PASMC proliferation was enhanced by Jag-1 and restored to normal levels by DAPT. Summarized data showing the total numbers of normal PASMCs and acute hypoxic PASMCs after culture in growth media for 48, 72 and 96 h ($n=3$ experiments). Data showing the inhibitory effects of the Notch3-siRNA on the proliferation of hypoxic PASMCs (**$P<0.01$ *vs.* control-siRNA; **a**). Summarized data showing the stimulatory effects of Jag-1 on the proliferation of normoxic PASMCs (**b**). Summarized data showing the inhibitory effects of DAPT on the proliferation of hypoxic PASMCs (**c**; **$P<0.01$, hypoxia+DAPT *vs.* hypoxia+vehicle; hypoxia+Jag-1 *vs.* hypoxia+vehicle).

pressure transducer catheter (Millar Instruments) inserted through the right jugular vein using the MPVS Ultra data acquisition system. The data were then recorded and analyzed with AD Instruments Lab Chart Pro 7.0 software, Suzhou, China.

Western blot

The cells were scraped in ice-cold 1× RIPA buffer (Bio-Rad Laboratories) supplemented with protease inhibitors (Roche Applied Science, Indianapolis, IN, USA) and incubated on ice for 15 min. The lysates were then centrifuged and the supernatant was collected. The protein concentrations were determined by the Bradford method (Bio-Rad Laboratories) using bovine serum albumin as a standard. Equal amounts of protein were resolved on sodium dodecyl sulfate-polyacrylamide gels followed by electrophoretic transfer onto nitrocellulose membranes (Bio-Rad Laboratories). The membranes were then probed with primary antibodies (anti-CaSR monoclonal antibody (MA1–934, 1:200; Thermo Scientific, Rockford, IL, USA) or Notch intracellular domain (NICD; 07-1232, Millipore, Temecula, CA, USA)) overnight at 4 °C, followed by incubation with the appropriate HRP-linked secondary antibody. The signal was detected with ECL substrate (Pierce Biotechnology, Rockford, IL, USA). Solubilized protein isolated from endothelium-denuded pulmonary arteries was loaded on an 8% acrylamide gel, transferred to an immobilon-P transfer membrane (Millipore, Bedford, MA, USA) and immunoblotted with an anti-CaSR monoclonal antibody (MA1–934,1:200; Thermo Scientific) or NICD (07-1232, Millipore, Temecula, CA, USA). The signals were detected using a Super Signal West Pico Chemiluminescent Substrate (Thermo Scientific). The protein levels were normalized to β-actin (sc-81178, Santa Cruz, CA, USA) and are expressed in arbitrary units.

Real-time PCR

The extraction of total RNA from the rat PASMCs and the reverse transcription reactions were performed with TRIzol Reagent (Invitrogen, Carlsbad, CA, USA) and the High Capacity cDNA Reverse Transcription Kit (Applied Biosystems, Foster City, CA, USA), respectively. Quantitative real-time PCR analysis was performed based on the SYBR assay (SYBR Green Master Mix; Roche) using gene-specific primers for rat CaSR and GAPDH on a Bio-Rad CFX384 Real-Time System C1000 Thermal Cycler system (Bio-Rad Laboratories). The CaSR mRNA was detected using real-time PCR 48 h after the PASMCs were treated with DAPT or Jag-1.

Transfection of small interfering RNAs

PASMCs were transiently transfected with a control small interfering RNA (siRNA) (50 nmol l^{-1}, Santa Cruz Biotechnology) or a Notch3-siRNA (50 nmol l^{-1}, Santa Cruz Biotechnology) using an Amaxa Basic Nucleofector kit for primary smooth muscle cells (Lonza, Suzhou, China). The $[Ca^{2+}]_{cyt}$ measurements and western blots of the siRNA-transfected cells were performed 48 to 72 h after electroporation. The cells were transfected with 100 nmol l^{-1} siRNA in Opti-MEM (Invitrogen) using Lipofectamine 2000 (Invitrogen), according to the manufacturer's recommendation.

Hematoxylin and eosin staining

The left lung lobes were fixed in a 3% paraformaldehyde solution and embedded in paraffin. Hematoxylin and eosin staining was performed on 3 μm sections using common histopathological procedures.

Assessment of RV hypertrophy and myocardial fibrosis

The RV hypertrophy was expressed as the ratio of weight of the RV wall and the weight of the free LV (left ventricular) wall and ventricular septum (LV+S). The

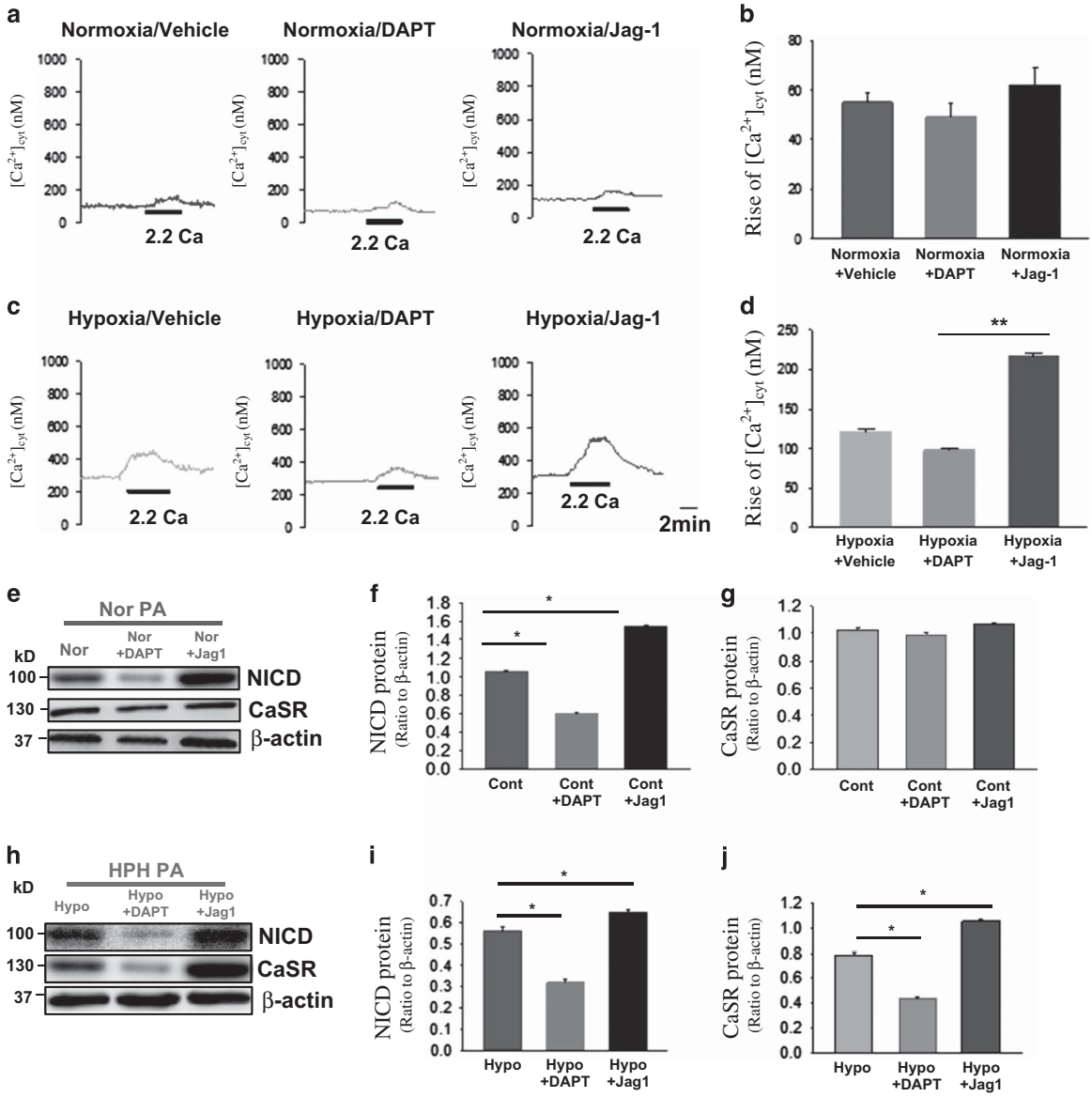

Figure 4 The extracellular Ca^{2+}-induced increase in $[Ca^{2+}]_{cyt}$ in freshly isolated pulmonary arterial smooth muscle cells (PASMCs) from the HPH rats is enhanced by the Jag-1 treatment *in vivo* and restored to normal levels by the injection with DAPT. The treatment with Jag-1 significantly enhanced the increased $[Ca^{2+}]_{cyt}$ in hypoxic PASMCs *in vivo*. The DAPT treatment significantly restored the increased $[Ca^{2+}]_{cyt}$ in hypoxic PASMCs *in vivo* (**c** and **d**). No differences in the increased $[Ca^{2+}]_{cyt}$ observed between normoxia+vehicle, normoxia+Jag-1 and normoxia+DAPT groups (**a** and **b**). The expression of the Ca^{2+}-sensing receptor (CaSR) protein in the hypoxia+Jag-1 group was significantly increased compared with the hypoxia+vehicle group (**h** and **j**). The expression of the CaSR protein in the hypoxia+DAPT group was significantly decreased compared with the hypoxia+vehicle (**h** and **j**). The expression of the Notch intracellular domain (NICD) protein was increased by Jag-1 and decreased by DAPT (**e**–**g** and **i**). No differences were observed between the normoxia+vehicle and normoxia+DAPT groups or between the normoxia+vehicle and normoxia+Jag-1 groups (**e**), $^{**}P<0.01$ *vs.* vehicle. A full color version of this figure is available at *Hypertension Research* online.

RV wall was separated from the LV wall and ventricular septum. Wet weights of the RV, free LV wall and ventricular septum were determined. Formalin-fixed and paraffin-embedded sections (3 μm) were generated from the right ventricles of rats and mice. Masson's trichrome staining was performed to examine the right ventricular myocardial fibrosis.

Assessment of the pulmonary artery thickness

The left lung lobes (from rats or mice) were fixed in a 3% paraformaldehyde solution, and the lobes were dissected in the middle and embedded in paraffin. All paraffin-embedded tissue blocks were sectioned at 3 μm. Hematoxylin and eosin staining was performed using common histopathological procedures. Histological analysis was performed in a blinded manner; the person who dissected the lobes coded the tissue blocks with numbers and gave them to another person to analyze the pulmonary vascular wall thickness. Microscopic images were analyzed using a computerized morphometric system (Aperio Imagescope v11.1.2.752 software) to assess the pulmonary arterial wall thickness. Pulmonary arteries were categorized according to their external diameter: category 1 includes the arteries with an external diameter between 25 and 50 μm; category 2 includes the arteries with an external diameter between 51 and 100 μm; and category 3 includes the arteries with an external diameter greater than 100 μm. The thickness of an artery was determined by the average values obtained in multiple areas of the artery.

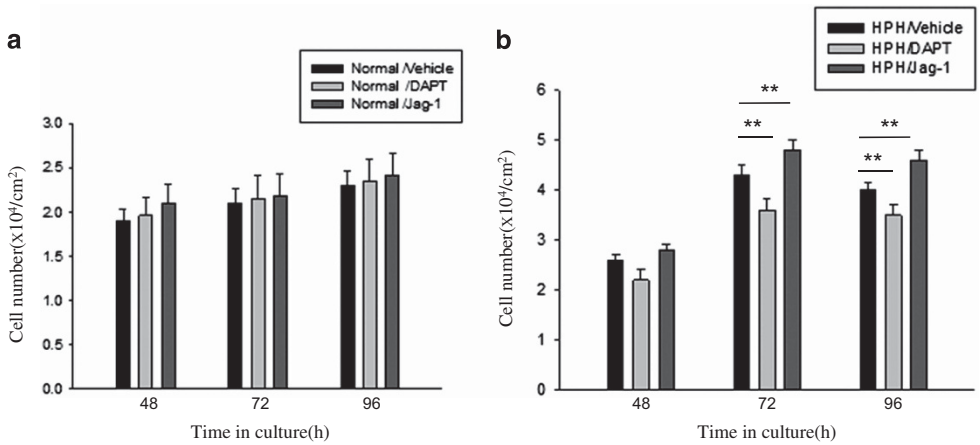

Figure 5 The proliferation of freshly isolated pulmonary arterial smooth muscle cells (PASMCs) from the HPH rats is enhanced by Jag-1 and restored to normal levels by DAPT. Summarized data showing the stimulatory effects of Jag-1 on the proliferation of freshly isolated PASMCs from the normal rats (**a**). Summarized data showing the inhibitory effects of DAPT on the proliferation of freshly isolated PASMCs from the HPH rats (**b**; $^{**}P<0.01$, hypoxia+DAPT *vs.* hypoxia+vehicle; hypoxia+Jag-1 *vs.* hypoxia+vehicle).

Statistical analysis

Composite data are shown as the mean ± s.e. The statistical significance of the differences between two groups was determined by Student's *t*-test. The statistical significance of the differences among groups was determined by one-way analysis of variance followed by Scheffe's test. Significant difference is expressed as $P<0.05$ or $P<0.01$.

RESULTS

The extracellular Ca^{2+}-induced increase in $[Ca^{2+}]_{cyt}$ in acute hypoxic rat PASMCs was enhanced by Jag-1 and restored to normal levels by a γ-secretase inhibitor (DAPT)

We first examined and compared the effects of extracellular Ca^{2+} restoration on changes in $[Ca^{2+}]_{cyt}$ in PASMCs from the normoxia +vehicle, normoxia+DAPT, normoxia+Jag-1, hypoxia+vehicle, hypoxia+DAPT and hypoxia+Jag-1 groups ($n=3$ experiments). The Jag-1 treatment significantly increased the increased $[Ca^{2+}]_{cyt}$ in hypoxic PASMCs *in vitro*. The DAPT treatment significantly decreased the increased $[Ca^{2+}]_{cyt}$ in hypoxic PASMCs *in vitro* (Figures 1c and d). No differences were observed in the increased $[Ca^{2+}]_{cyt}$ between normoxia+vehicle, normoxia+Jag-1 and normoxia+DAPT (Figures 1a and b). Real-time PCR analyses of CaSR in PASMCs were performed 48 h after the DAPT or Jag-1 treatments. The expression of the CaSR mRNA was increased by Jag-1 and decreased by DAPT, but only in the hypoxic condition (Figures 1k and l). The expression of the CaSR protein in the hypoxia+Jag-1 group was significantly increased compared with the hypoxia+vehicle group (Figures 1h and j). The expression of the CaSR protein in hypoxia+DAPT group was significantly reduced compared with the hypoxia+vehicle group (Figures 1h and j). The expression of the NICD protein was increased by Jag-1 and decreased by DAPT (Figures 1e–g and i). No differences were observed between the normoxia+vehicle and normoxia+DAPT groups or between the normoxia+vehicle and normoxia+Jag-1 groups (Figure 1e); $^{**}P<0.01$ *vs.* vehicle.

Downregulation of Notch3 with a siRNA attenuates the extracellular Ca^{2+}-induced increase in $[Ca^{2+}]_{cyt}$ and the increase in hypoxia-induced PASMC proliferation in acute hypoxic rat PASMCs

We also examined and compared the effects of extracellular Ca^{2+} restoration on the changes in $[Ca^{2+}]_{cyt}$ in PASMCs by downregulating Notch3 with a siRNA. Representative records of the $[Ca^{2+}]_{cyt}$ changes and the summarized data showed the extracellular Ca^{2+}-induced increases in $[Ca^{2+}]_{cyt}$ in normoxic PASMCs transfected with the control-siRNA ($n=52$) and Notch3-siRNA ($n=53$; Figures 2a and b). Representative records of the $[Ca^{2+}]_{cyt}$ changes and the summarized data showed the extracellular Ca^{2+}-induced $[Ca^{2+}]_{cyt}$ increases in acute hypoxic PASMCs transfected with the control-siRNA ($n=55$) and Notch3-siRNA ($n=57$); $^{**}P<0.01$ *vs.* control-siRNA (Figures 2c and d). Western blots and analysis of the summarized data of the NICD and CaSR levels in normoxic and hypoxic PASMCs treated with a control (or scrambled) siRNA (control) and Notch3-siRNA were shown (at 25 and 50 nmol l^{-1}, $n=3$ for each group; Figures 2e–g). The summarized data show the total numbers of normal PASMCs and acute hypoxic PASMCs after culture in growth media for 48, 72 and 96 h ($n=3$ experiments). The data show the inhibitory effects of the Notch3-siRNA on the proliferation of hypoxic PASMCs ($^{**}P<0.01$ *vs.* control-siRNA; Figure 3a).

Hypoxia-induced PASMC proliferation was enhanced by Jag-1 and restored to normal levels by DAPT

The summarized data (the mean ± s.e., $n=3$ experiments) showed the stimulatory effects of Jag-1 on normoxic PASMC proliferation (Figure 3b). The summarized data (the mean ± s.e., $n=3$ experiments) showed the inhibitory effects of DAPT on hypoxic PASMC proliferation (Figure 3c; $^{**}P<0.01$, hypoxia+DAPT *vs.* hypoxia+vehicle; hypoxia+Jag-1 *vs.* hypoxia+vehicle).

The extracellular Ca^{2+}-induced increase in $[Ca^{2+}]_{cyt}$ in freshly isolated PASMCs from the HPH rats was enhanced by the Jag-1 treatment *in vivo* and restored to normal levels by an injection with DAPT

We also examined and compared the effects of extracellular Ca^{2+} restoration on the changes in $[Ca^{2+}]_{cyt}$ in freshly isolated PASMCs from normoxia+vehicle, normoxia+DAPT, normoxia+Jag-1, hypoxia+vehicle, hypoxia+DAPT and hypoxia+Jag-1 groups *in vivo* ($n=6$ per group). The Jag-1 treatment significantly increased the increased $[Ca^{2+}]_{cyt}$ in hypoxic PASMCs *in vivo*. The DAPT treatment significantly decreased the increased $[Ca^{2+}]_{cyt}$ in hypoxic PASMCs *in vivo* (Figures 4c and d). No differences in the increased $[Ca^{2+}]_{cyt}$ were observed between the normoxia

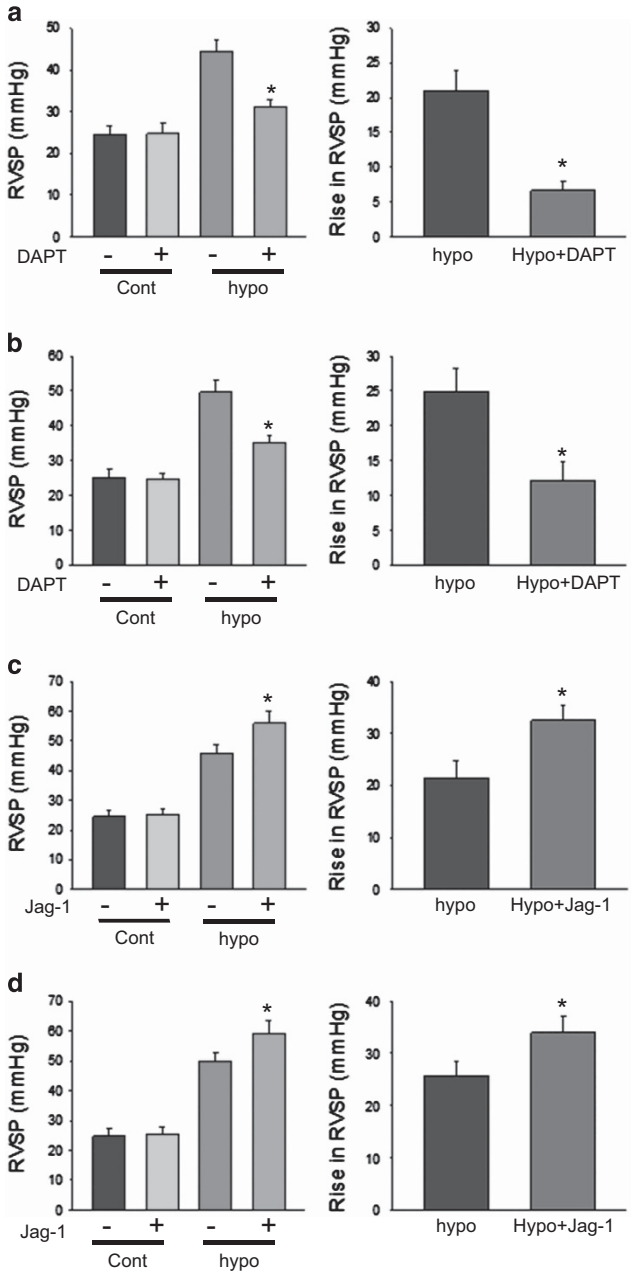

Figure 6 Hemodynamic changes in the HPH rats after the DAPT and Jag-1 treatments. Summarized data showing that DAPT not only prevented (**a**) but also rescued (**b**) the increase in right ventricular systolic pressure (RVSP) in the HPH rats (*$P<0.05$, HPH+DAPT *vs.* HPH). Jag-1 enhanced the increase in RVSP in both the prevention (**c**) and rescue (**d**) experiments (*$P<0.05$, HPH+Jag-1 *vs.* HPH). A full color version of this figure is available at *Hypertension Research* online.

+vehicle, normoxia+Jag-1 and normoxia+DAPT groups (Figures 4a and b). The expression of the CaSR protein in the hypoxia+Jag-1 group was significantly increased compared with the hypoxia+vehicle group (Figures 4h and j). The expression of the CaSR protein in hypoxia+DAPT group was significantly decreased compared with the hypoxia+vehicle (Figures 4h and j). The expression of the NICD protein was increased by Jag-1 and decreased by DAPT (Figures 4e–g and i). No differences were observed between the normoxia+vehicle and normoxia+DAPT

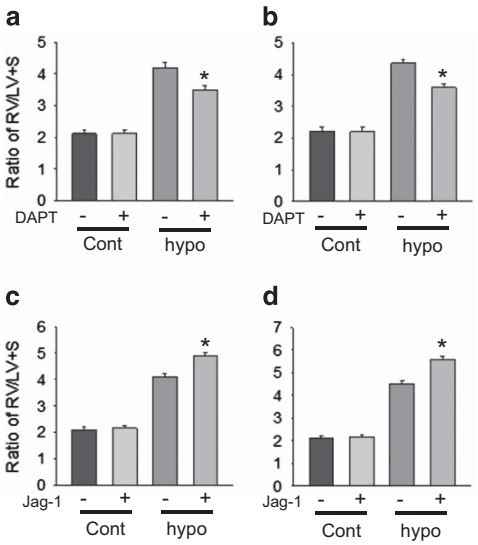

Figure 7 Changes in right ventricular hypertrophy in the HPH rats after the DAPT and Jag-1 treatments. Summarized data showing that DAPT not only prevented (**a**) but also rescued (**b**) the increase in the average Fulton index [RV/(LV+S) ratio, means+s.e.] in the HPH rats (*$P<0.05$, HPH+DAPT *vs.* HPH). Jag-1 enhanced the increase in the RV/(LV+S) ratio in both the prevention (**c**) and rescue (**d**) experiments (*$P<0.05$, HPH+Jag-1 *vs.* HPH). A full color version of this figure is available at *Hypertension Research* online.

groups or between the normoxia+vehicle and normoxia+Jag-1 groups (Figure 4e; **$P<0.01$ *vs.* vehicle).

The proliferation of freshly isolated PASMCs from the HPH rats was enhanced by Jag-1 and restored to normal levels by DAPT

The summarized data showed the stimulatory effects of Jag-1 on the proliferation of freshly isolated PASMCs from the normal rats (Figure 5a). The summarized data showed the inhibitory effects of DAPT on the proliferation of freshly isolated PASMCs from the HPH rats (Figure 5b; **$P<0.01$, hypoxia+DAPT *vs.* hypoxia+vehicle; hypoxia+Jag-1 *vs.* hypoxia+vehicle).

Hemodynamic changes in the HPH rats after the DAPT or Jag-1 treatments

The summarized data ($n=6$ per group) showed that DAPT not only prevented (Figure 6a) but also rescued (Figure 6b) the increase in RVSP in the HPH rats (*$P<0.05$, HPH+DAPT *vs.* HPH). Jag-1 enhanced the increase in RVSP in both the prevention experiments (Figure 6c) and the rescue experiments (Figure 6d; *$P<0.05$, HPH +Jag-1 *vs.* HPH).

Changes in right ventricular hypertrophy in the HPH rats after the DAPT or Jag-1 treatments

The summarized data ($n=6$ per group) showed that DAPT not only prevented (Figure 7a) but also rescued (Figure 7b) the increase in the average Fulton index [RV/(LV+S) ratio, means+s.e.] in the HPH rats (*$P<0.05$, HPH+DAPT *vs.* HPH). Jag-1 enhanced the increase in the RV/(LV+S) ratio in both the prevention experiments (Figure 7c) and the rescue experiments (Figure 7d; *$P<0.05$, HPH+Jag-1 *vs.* HPH).

Changes in right ventricular myocardial fibrosis in the HPH rats after the DAPT or Jag-1 treatments

Representative images of Masson's trichrome staining (Figures 8a–d) and the summarized data (Figure 8i) showed that DAPT (days 1–14)

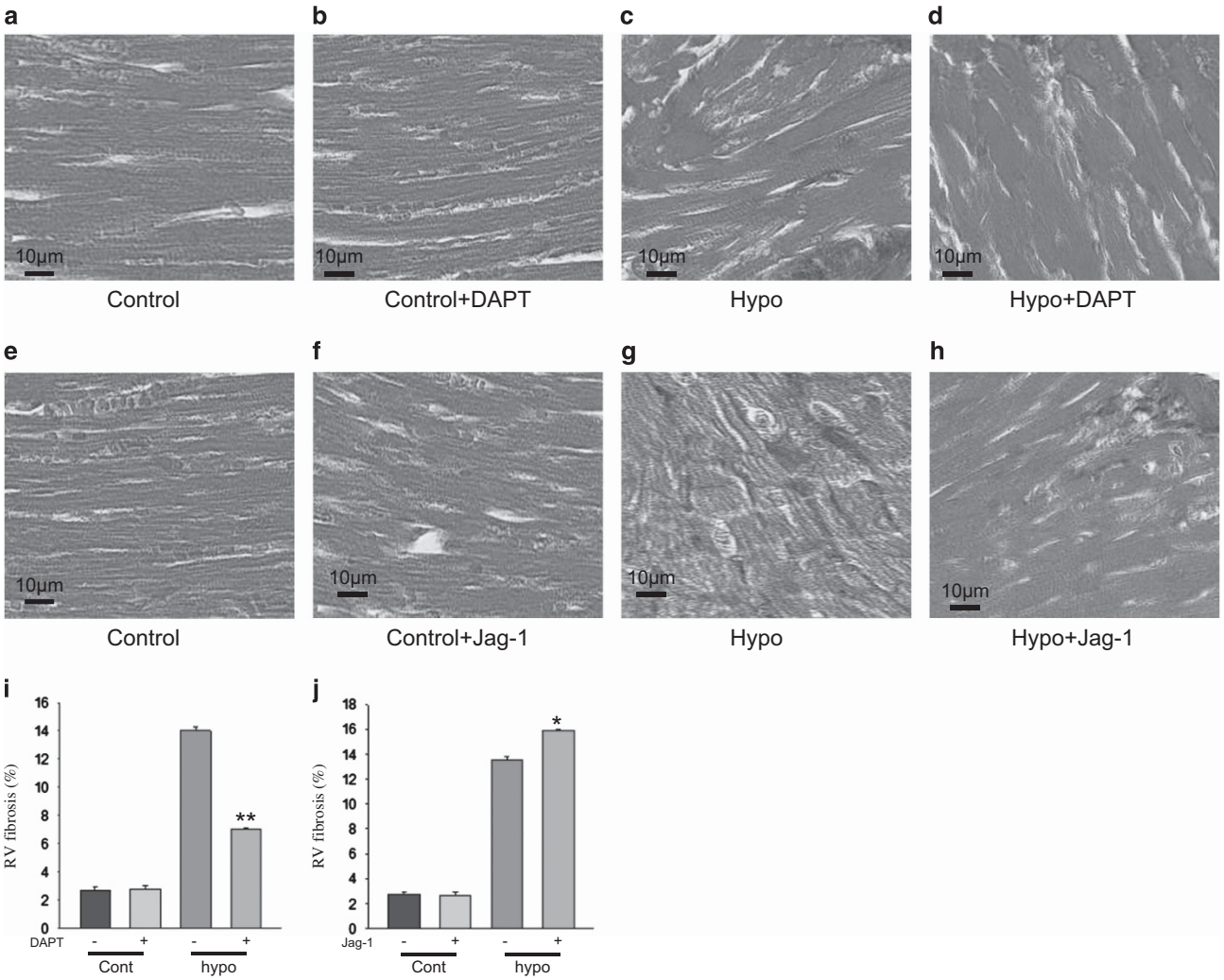

Figure 8 The DAPT and Jag-1 treatments change the development of right ventricular myocardial fibrosis in the HPH rats in the prevention experiments. Representative images of Masson's trichrome staining (**a**–**d**) showing that DAPT (days 1–14) attenuate myocardial fibrosis in the right ventricles from the HPH rats. The value of right ventical fibrosis (%) in hypo+DAPT group (days 1–14) is almost half of that in hypoxia alone group (Summarized data in Panel **i**). $^{**}P<0.01$ *vs.* hypoxia alone. Representative images of Masson's trichrome staining (**e**–**h**) and summarized data (**j**) showing that Jag-1 (days 1–14) increased myocardial fibrosis in the right ventricles from the HPH rats. $^{*}P<0.05$ *vs.* hypoxia alone. A full color version of this figure is available at *Hypertension Research* online.

attenuated myocardial fibrosis in the right ventricles from the HPH rats ($n=6$ per group). Representative images of Masson's trichrome staining (Figures 8e–h) and the summarized data (Figure 8j) showed that Jag-1 (days 1–14) increased myocardial fibrosis in the right ventricles from the HPH rats ($^{*}P<0.05$ *vs.* hypoxia alone; $^{**}P<0.01$ *vs.* hypoxia alone).

Representative images of Masson's trichrome staining (Figures 9a–d) and the summarized data (Figure 9i) showed that DAPT (days 14–24) attenuated myocardial fibrosis in the right ventricles from the HPH rats ($n=6$, each group). Representative images of Masson's trichrome staining (Figures 9e–h) and the summarized data (Figure 9j) showed that Jag-1 (days 14–24) increased myocardial fibrosis in the right ventricles from the HPH rats ($^{*}P<0.05$ *vs.* hypoxia alone; $^{**}P<0.01$ *vs.* hypoxia alone).

The DAPT and Jag-1 treatments change the development of pulmonary vascular remodeling in HPH rats

DAPT (days 1–14) attenuated pulmonary vascular remodeling in the HPH rats (Figure 10a). Jag-1 (days 1–14) increased pulmonary vascular remodeling in the HPH rats (Figure 10c). Summarized data of the medial thickness of pulmonary arteries with diameters (Ø) of less than 50 μm, between 50 and 100 μm and greater than 100 μm in normal control rats and HPH rats that were treated with vehicle, DAPT or Jag-1 were shown ($n=6$ per group; $^{**}P<0.05$ *vs.* hypoxia alone; Figures 10b and d). DAPT (days 14–24) attenuated pulmonary vascular remodeling in the HPH rats (Figure 11a). Jag-1 (days 14–24) increased pulmonary vascular remodeling in the HPH rats (Figure 11c). Summarized data of the medial thickness of pulmonary arteries with diameters (Ø) of less than 50 μm, between 50 and 100 μm and greater than 100 μm in the normal control rats and the HPH rats that were treated with vehicle, DAPT or Jag-1 were shown ($n=6$ per group; $^{**}P<0.05$ *vs.* hypoxia alone; Figures 11b and d).

DISCUSSION

In this study, we found that (1) acute hypoxia activates Notch signaling and enhances CaSR function, (2) hypoxia activates Notch signaling and increases CaSR expression, (3) chronic hypoxia activates Notch signaling, which upregulates and actives CaSR in HPH, (4) Jag-

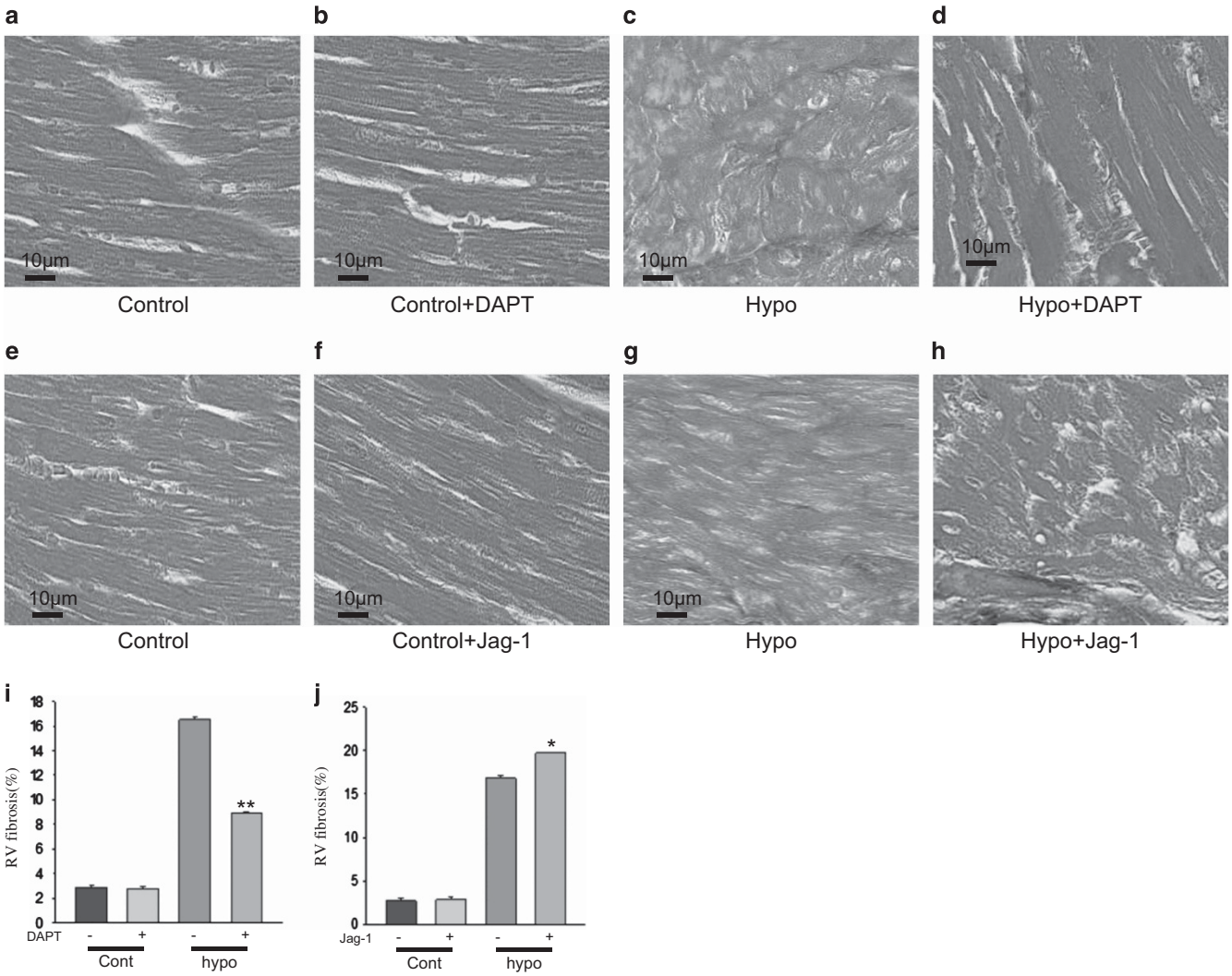

Figure 9 The DAPT and Jag-1 treatments change the development of right ventricular myocardial fibrosis in the HPH rats in the rescue experiments. Representative images of Masson's trichrome staining (**a**–**d**) showing that DAPT (days 14–24) attenuated myocardial fibrosis in the right ventricles from the HPH rats. The value of right ventical fibrosis (%) in hypo+DAPT group (days 14–24) is almost half of that in hypoxia alone group (Summarized data in Panel **i**). $^{**}P<0.01$ *vs.* hypoxia alone. Representative images of Masson's trichrome staining (**e**–**h**) and summarized data (**j**) showing that Jag-1 (days 14–24) increased myocardial fibrosis in the right ventricles from the HPH rats. $^{*}P<0.05$ *vs.* hypoxia alone. A full color version of this figure is available at *Hypertension Research* online.

1 activates Notch signaling and increases the RVSP and vascular remodeling in HPH rats, (5) Notch3 downregulation attenuates the function of CaSR and decreases CaSR expression in hypoxic PASMCs and (6) pharmacological blockade of Notch signaling with DAPT (a γ-secretase inhibitor) prevents and inhibits the development of HPH in rats. Collectively, these data imply that hypoxia-induced activation of Notch signaling enhances extracellular Ca^{2+}-induced increase in $[Ca^{2+}]_{cyt}$ by activating and upregulating CaSR, leading to the development of HPH. This study is the first to report that Notch activation of CaSR mediates the development of HPH.

The Notch signaling pathway is an evolutionarily conserved pathway that dictates cell fate and influences cell proliferation, differentiation and apoptosis.[29,30] Both Notch receptors (Notch1–Notch4) and their ligands, Jagged (Jag-1 and Jag-2) and Delta-like (Dll1, Dll3 and Dll4), are single transmembrane-spanning proteins that restrict Notch signaling to adjacent cells. After ligand binding, Notch undergoes a series of proteolytic cleavages, resulting in the release of NICD, which translocates to the nucleus where it interacts with RBP-Jκ to function as a transcription factor.[23,31–33] The activation of Notch receptors by their ligands leads to the cleavage of[33] the NICD in the cytosol by γ-secretase; NICD then translocates into[34] the nucleus to regulate gene transcription. On entering the nucleus, NICD binds RBP-Jκ and displaces the co-repressor complex. This displacement leads to the recruitment of the transcriptional co-activator Mastermind-like 1 and histone acetyltransferases, resulting in the transcription of Notch target genes.[22,31–33] On activation by Notch, the transcriptional repressors Hes and Hey reduce the expression of downstream targets, such as Mash,[34] myoD[35] and myocardin,[36] as well as the cell cycle proteins $p27^{kip1}$ (ref. 37) and $p21^{waf/cip1}$.[38]

Notch signaling is also important for regulating the growth, apoptosis, migration and differentiation of vascular smooth muscle cells[39–41] and is a key mediator of vascular morphogenesis.[42–44] Notch3 is only expressed in vascular smooth muscle cells of arteries, but not veins.[23] We have previously demonstrated that Notch3 is upregulated in patients with pulmonary hypertension and in animal models of experimental pulmonary hypertension.[24]

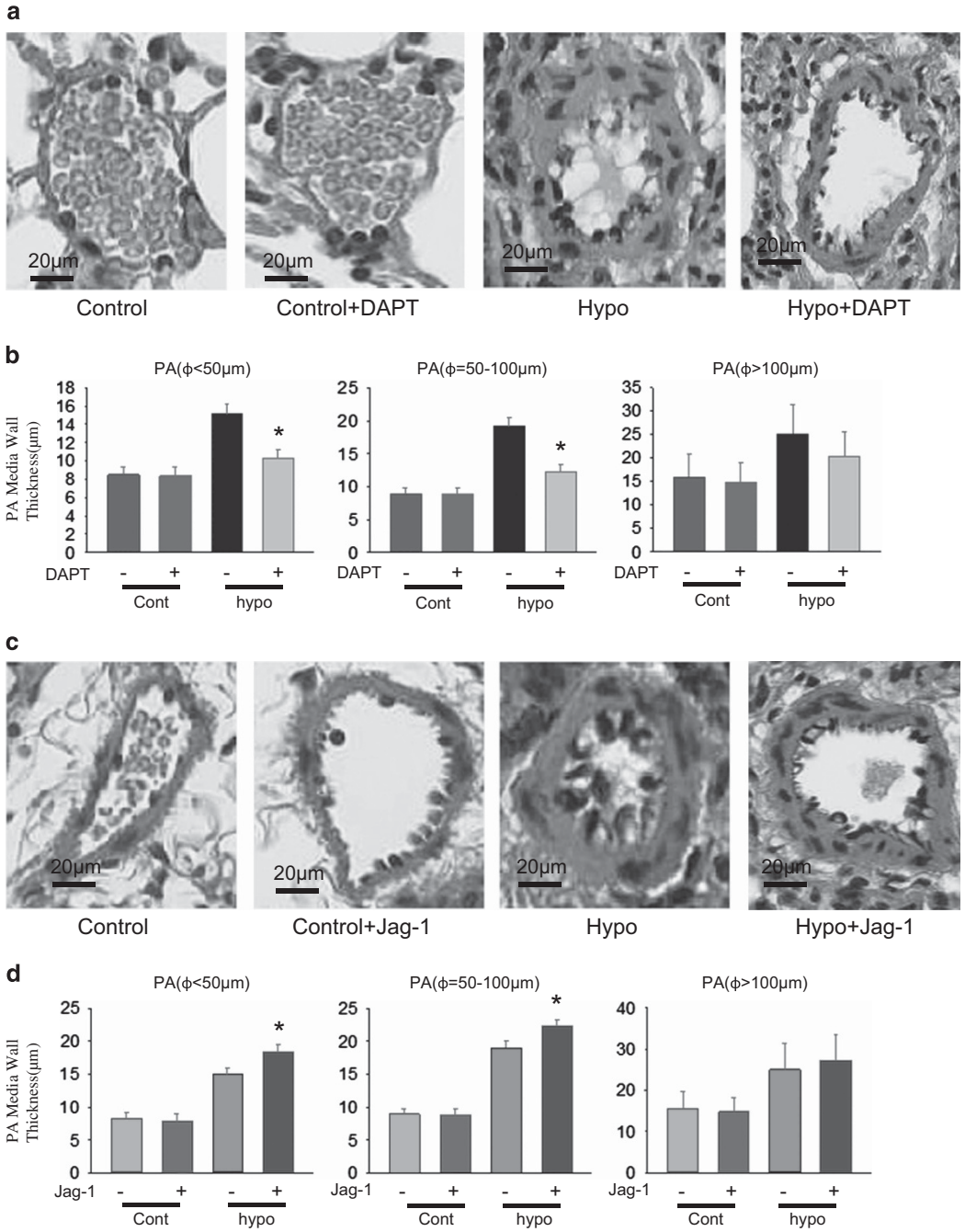

Figure 10 The DAPT and Jag-1 treatments change the development of pulmonary vascular remodeling in the HPH rats in the prevention experiments. Representative images of hematoxylin and eosin staining in small pulmonary arteries. DAPT (days 1–14) attenuated pulmonary vascular remodeling in the HPH rats (**a**). Jag-1 (days 1–14) increased pulmonary vascular remodeling in the HPH rats (**c**). Summarized data showing the medial thickness of the pulmonary arteries with diameters (Ø) of less than 50 μm, between 50 and 100 μm and greater than 100 μm in the normal control rats and HPH rats that were treated with vehicle, DAPT or Jag-1. $*P<0.05$ *vs.* hypoxia alone (**b** and **d**). A full color version of this figure is available at *Hypertension Research* online.

In this study, we show that hypoxia-mediated Notch signaling has effects on the functional activation and upregulation of CaSR, which are associated with the development of pulmonary vascular remodeling in HPH. It has previously been shown that hypoxia requires Notch signaling to maintain cells in an undifferentiated state.[45] Hypoxia induces PASMC proliferation, and these proliferating PASMCs exhibit an undifferentiated phenotype.[46,47] PASMCs are not terminally differentiated, and Notch signaling controls PASMC differentiation and modulates the expression of contractile genes.[36,48–50] Vascular remodeling, which is partially caused by increased PASMC proliferation, contributes to the increased pulmonary vascular resistance in HPH. A recent study from our group showed that NICD directly interacts with and activates transient receptor potential (TRP) 6, leading to enhanced store-operated Ca^{2+} entry and an increase in $[Ca^{2+}]_{cyt}$ in PASMCs. The results suggest that the interaction of NICD and TRPC6 is independent of any transcriptional functions of Notch

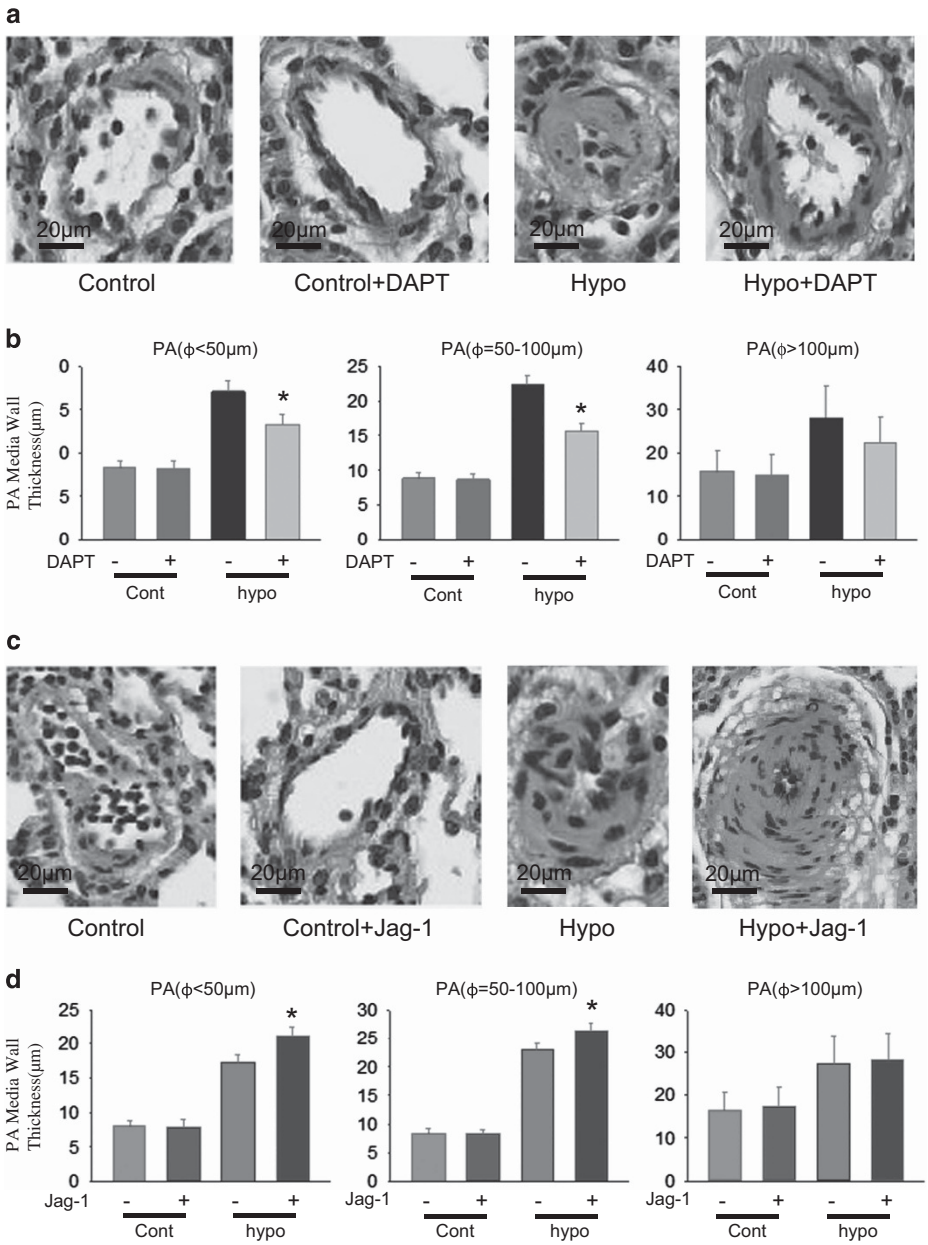

Figure 11 The DAPT and Jag-1 treatments change the development of pulmonary vascular remodeling in the HPH rats in the rescue experiments. Representative images of hematoxylin and eosin staining of small pulmonary arteries. DAPT (Days 14–24) attenuated pulmonary vascular remodeling in the HPH rats (**a**). Jag-1 (Days 14–24) increased pulmonary vascular remodeling in the HPH rats (**c**). Summarized data showing the medial thickness of the pulmonary arteries with diameters (Ø) of less than 50 μm, between 50 and 100 μm and greater than 100 μm in the normal control rats and HPH rats that were treated with vehicle, DAPT or Jag-1. $^*P<0.05$ *vs.* hypoxia alone (**b** and **d**). A full color version of this figure is available at *Hypertension Research* online.

signaling. Several studies have described cross-talk between TRP and Notch. Previous studies in neuronal cells have reported NICD-dependent transcription of TRPC6,[51] and TRPC6 is a key mediator of the Notch-driven growth and invasion of glioblastoma cells.[52] It has been reported that CaSR[53] and TRPC channels co-regulated the intracellular Ca^{2+} concentrations.[54] Together, these findings support our hypothesis that CaSR mediates the pulmonary vascular remodeling observed in HPH via Notch signaling.

These data suggest that Notch signaling contributes to the regulation of CaSR function in PASMCs. The enhancement of CaSR function in PH may occur via two different mechanisms: (a) a direct functional interaction of NICD with CaSR and/or its possible regulatory proteins and (b) our PCR and siRNA data suggest that Notch signaling potentially upregulates the transcription of genes encoding the CaSR proteins in PASMCs. Expression of Jag-1 in the pulmonary artery has been well studied, due to its association with Alagille Syndrome, which is caused by a Jag-1 mutation. Patients with Alagille Syndrome have major abnormalities in their pulmonary arteries resulting from inactivating mutations in Jag-1.[52,55]

The specific aim of this study was to determine CaSR function and expression following the activation or pharmacological blockade of Notch signaling to further understand the role of CaSR in the

mechanism of PH. We examined this pathway and showed that Jag-1 increased the extracellular Ca^{2+}-induced increases in $[Ca^{2+}]_{cyt}$ in freshly isolated primary PASMCs from the HPH rats. Western blot analysis was carried out on pulmonary arteries from the HPH rats to test the effect of Jag-1 on CaSR expression in these arteries. We found that the Jag-1 treatment increased CaSR expression in the HPH rats. Importantly, we found that Notch3 downregulation attenuated the function of CaSR and decreased CaSR expression in hypoxic PASMCs. In addition, the pharmacological prevention and rescue effects of DAPT on PH was examined in HPH rats. Our data show that Jag-1 increases RVSP, right ventricular hypertrophy and right ventricular myocardial fibrosis in HPH rats. DAPT either partially or fully prevents and rescues HPH in rats. These results will help identify the interplay between CaSR function and the phenotype of PH, illustrating that Notch-mediated activation may be a novel target for future clinical treatments.

In conclusion, these data suggest that hypoxia activates Notch signaling to upregulate and active CaSR, contributing to the development of HPH. Our data provide compelling evidence that Notch signaling is potentially involved in regulating CaSR function in PH. The mechanisms responsible for the stimulatory effect of Notch signaling on CaSR in PASMCs may include (a) a direct functional interaction of NICD with the CaSR and/or its regulatory proteins and (b) potential transcriptional upregulation of genes encoding the CaSR proteins in PASMCs. Elucidation of the sequence of events underlying the Notch-mediated enhancement of Ca^{2+} signaling in PASMCs will provide critical insights and an in-depth understanding of the pathogenic mechanisms of PAH. The originality of this study is not only in the identification of the involvement of Notch signaling and CaSR in regulating $[Ca^{2+}]_{cyt}$ but will also provide a new concept for the design of combination therapies for the treatment of HPH.

CONFLICT OF INTEREST

The authors declare no conflict of interest.

ACKNOWLEDGEMENTS

This work was supported by grants from the National Natural Science Foundation of China (NSFC81300040), the Natural Science Foundation of Jiangsu Province (BK20141184), the China National Clinical Key Subject and Application Foundation of Suzhou China (SYS201336) and the Six talent peaks project in Jiangsu Province (WSN021).

1 Yuan XJ, Rubin LJ. Pathogenesis of pulmonary arterial hypertension: the need for multiple hits. *Circulation* 2005; **111**: 534–538.
2 Sun XQ, Zhang R, Zhang HD, Yuan P, Wang XJ, Zhao QH, Wang L, Jiang R, Jan Bogaard H, Jing ZC. Reversal of right ventricular remodeling by dichloroacetate is related to inhibition of mitochondria-dependent apoptosis. *Hypertens Res* 2016; **39**: 302–311.
3 Yun X, Chen Y, Yang K, Wang S, Lu W, Wang J. Upregulation of canonical transient receptor potential channel in the pulmonary arterial smooth muscle of a chronic thromboembolic pulmonary hypertension rat model. *Hypertens Res* 2015; **38**: 821–828.
4 Jiang R, Ai ZS, Jiang X, Yuan P, Liu D, Zhao QH, He J, Wang L, Gomberg-Maitland M, Jing ZC. Intravenous fasudil improves in-hospital mortality of patients with right heart failure in severe pulmonary hypertension. *Hypertens Res* 2015; **38**: 539–544.
5 Castaldi PJ, Hersh CP, Reilly JJ, Silverman EK. Genetic associations with hypoxemia and pulmonary arterial pressure in COPD. *Chest* 2009; **135**: 737–744.
6 Voelkel NF, Cool CD. Pulmonary vascular involvement in chronic obstructive pulmonary disease. *Eur Respir J Suppl* 2003; **46**: 28s–32s.
7 Moudgil R, Michelakis ED, Archer SL. Hypoxic pulmonary vasoconstriction. *J Appl Physiol* 2005; **98**: 390–403.
8 Morrell NW, Adnot S, Archer SL, Dupuis J, Jones PL, MacLean MR, McMurtry IF, Stenmark K, Thistlethwaite PA, Weissmann N, Yuan XJ, Weir EK. Cellular and molecular basis of pulmonary arterial hypertension. *J Am Coll Cardiol* 2009; **54**: S20–S31.
9 Yamamura A, Guo Q, Yamamura H, Zimnicka AM, Pohl NM, Smith KA, Fernandez RA, Zeifman A, Makino A, Dong H, Yuan JX. Enhanced Ca^{2+}-sensing receptor function in idiopathic pulmonary arterial hypertension. *Circ Res* 2012; **111**: 469–481.
10 Yamamura A, Yamamura H, Zeifman A, Yuan JX-J. Activity of Ca^{2+}-activated Cl^-channels contributes to regulating receptor- and store operated Ca^{2+} entry in human pulmonary artery smooth muscle cells. *Pulm Circ* 2011; **1**: 269–279.
11 Berry MF, Engler AJ, Woo YJ, Pirolli TJ, Bish LT, Jayasankar V, Morine KJ, Gardner TJ, Discher DE, Sweeney HL. Mesenchymal stem cell injection after myocardial infarction improves myocardial compliance. *Am J Physiol Heart Circ Physiol* 2006; **290**: H2196–H2203.
12 Hassoun PM, Mouthon L, Barbera´ JA. Inflammation, growth factors, and pulmonary vascular remodeling. *J Am Coll Cardiol* 2009; **54**: S10–S19.
13 Firth AL, Remillard CV, Yuan JX. Trp channels in hypertension. *Biochim Biophys Acta* 2007; **1772**: 895–906.
14 Zhang S, Patel HH, Murray F, Remillard CV, Schach C, Thistlethwaite PA, Insel PA, Yuan JX. Pulmonary artery smooth muscle cells from normal subjects and IPAH patients show divergent camp-mediated effects on TRPC expression and capacitative Ca^{2+} entry. *Am J Physiol Lung Cell Mol Physiol* 2007; **292**: L1202–L1210.
15 Yu Y, Keller SH, Remillard CV. A functional single-nucleotide polymorphism in the trpc6 gene promoter associated with idiopathic pulmonary arterial hypertension. *Circulation* 2009; **119**: 2313–2322.
16 Hofer AM, Brown EM. Extracellular calcium sensing and signalling. *Nat Rev Mol Cell Biol* 2003; **4**: 530–538.
17 Brown EM, MacLeod RJ. Extracellular calcium sensing and extracellular calcium signaling. *Physiol Rev* 2001; **81**: 239–297.
18 Magno AL, Ward BK, Ratajczak T. The calcium-sensing receptor: a molecular perspective. *Endocr Rev* 2011; **32**: 3–30.
19 Brown EM, Butters R, Katz C, Kifor O. Neomycin mimics the effects of high extracellular calcium concentrations on parathyroid function in dispersed bovine parathyroid cells. *Endocrinology* 1991; **128**: 3047–3054.
20 Conigrave AD, Quinn SJ, Brown EM. L-amino acid sensing by the extracellular Ca^{2+}-sensing receptor. *Proc Natl Acad Sci USA* 2000; **97**: 4814–4819.
21 Gowen M, Stroup GB, Dodds RA, James IE, Votta BJ, Smith BR, Bhatnagar PK, Lago AM, Callahan JF, DelMar EG, Miller MA, Nemeth EF, Fox J. Antagonizing the parathyroid calcium receptor stimulates parathyroid hormone secretion and bone formation in osteopenic rats. *J Clin Invest* 2000; **105**: 1595–1604.
22 Riccardi D, Finney BA, Wilkinson WJ, Kemp PJ. Novel regulatory aspects of the extracellular Ca^{2+}-sensing receptor, car. *Pflugers Arch* 2009; **458**: 1007–1022.
23 Gridley T. Notch signaling in the vasculature. *Curr Top Dev Biol* 2010; **92**: 277–309.
24 Li X, Zhang X, Leathers R, Makino A, Huang C, Parsa P, Macias J, Yuan JX, Jamieson SW, Thistlethwaite PA. Notch3 signaling promotes the development of pulmonary arterial hypertension. *Nat Med* 2009; **15**: 1289–1297.
25 Yamamura H, Yamamura A, Ko EA, Pohl NM, Smith KA, Zeifman A, Powell FL, Thistlethwaite, Yuan JX. Activation of Notch signaling by short-term treatment with Jagged-1 enhances store-operated Ca^{2+} Entry in human pulmonary arterial smooth muscle cells. *Am J Physiol Cell Physiol* 2014; **306**: C871–C878.
26 Smith KA, Voiriot G, Tang H, Fraidenburg DR, Song S, Yamamura H, Yamamura A, Guo Q, Wan J, Pohl NM, Tauseef M, Bodmer R, Ocorr K, Thistlethwaite PA, Haddad GG, Powell FL, Makino A, Mehta D, Yuan JX. Notch activation of Ca^{2+} signaling in the development of hypoxic pulmonary vasoconstriction and pulmonary hypertension. *Am J Respir Cell Mol Biol* 2015; **53**: 355–367.
27 Yuan XJ, Goldman WF, Tod ML, Rubin LJ, Blaustein MP. Ionic currents in rat pulmonary and mesenteric arterial myocytes in primary culture and subculture. *Am J Physiol* 1993; **264**: L107–L115.
28 Marshall CMA, Verhoeven AJ, Marshall BE. Pulmonary artery Nadphoxidase is activated in hypoxic pulmonary vasoconstriction. *Am J Respir Cell Mol Biol* 1996; **15**: 633–644.
29 Artavanis-Tsakonas S, Rand MD, Lake RJ. Notch signaling: cell fate control and signal integration in development. *Science* 1999; **284**: 770–776.
30 Miele L, Osborne B. Arbiter of differentiation and death: Notch signaling meets apoptosis. *J Cell Physiol* 1999; **181**: 393–409.
31 Bray SJ. Notch signalling:a simple pathway becomes complex. *Nat Rev Mol Cell Biol* 2006; **7**: 678–689.
32 Kopan R, Ilagan MX. The canonical Notch signaling pathway: unfolding the activation mechanism. *Cell* 2009; **137**: 216–233.
33 Thistlethwaite PA, Li X, Zhang X. Notch signaling in pulmonary hypertension. *Adv Exp Med Biol* 2010; **661**: 279–298.
34 Delapompa JL, Wakeham A, Correia KM, Samper E, Brown S, Aguilera RJ, Nakano T, Honjo T, Mak TW, Rossant J, Conlon RA. Conservation of the Notch signalling pathway in mammalian neurogenesis. *Development* 1997; **124**: 1139–1148.
35 Kopan R, Nye JS, Weintraub H. The intracellular domain of mouse Notch: a constitutively activated repressor of myogenesis directed at the basic helix-loop-helix region of MyoD. *Development* 1994; **120**: 2385–2396.
36 Proweller A, Pear WS, Parmacek MS. Notch signaling represses myocardin-induced smooth muscle cell differentiation. *J Biol Chem* 2005; **280**: 8994–9004.
37 Havrda MC, Johnson MJ, O'Neill CF, Liaw L. A novel mechanism of transcriptional repression of p27kip1 through Notch/HRT2 signaling in vascular smooth muscle cells. *Thromb Haemost* 2006; **96**: 361–370.
38 Wang W, Prince CZ, Hu X, Pollman MJ. HRT1 modulates vascular smooth muscle cell proliferation and apoptosis. *Biochem Biophys Res Commun* 2003; **308**: 596–601.
39 Campos AH, Wang W, Pollman MJ, Gibbons GH. Determinants of Notch-3 receptor expression and signaling in vascular smooth muscle cells: implications in cell-cycle regulation. *Circ Res* 2002; **91**: 999–1006.

40 Morrow D, Sweeney C, Birney YA, Cummins PM, Walls D, Redmond EM, Cahill PA. Cyclic strain inhibits Notch receptor signaling in vascular smooth muscle cells *in vitro*. *Circ Res* 2005; **96**: 567–575.
41 Sakata Y, Xiang F, Chen Z, Kiriyama Y, Kamei CN, Simon DI, Chin MT. Transcription factor CHF1/Hey2 regulates neointimal formation *in vivo* and vascular smooth muscle proliferation and migration *in vitro*. *Arterioscler Thromb Vasc Biol* 2004; **24**: 2069–2074.
42 Alva JA, Iruela-Arispe ML. Notch signaling in vascular morphogenesis. *Curr Opin Hematol* 2004; **11**: 278–283.
43 Hirschi KK, Majesky MW. Smooth muscle stem cells. *Anat Rec A Discov Mol Cell Evol Biol* 2004; **276**: 22–33.
44 Krebs LT, Xue Y, Norton CR, Shutter JR, Maguire M, Sundberg JP, Gallahan D, Closson V, Kitajewski J, Callahan R, Smith GH, Stark KL, Gridley T. Notch signaling is essential for vascular morphogenesis in mice. *Genes Dev* 2000; **14**: 1343–1352.
45 Gustafsson MV, Zheng X, Pereira T, Gradin K, Jin S, Lundkvist J, Ruas JL, Poellinger L, Lendahl U, Bondesson M. Hypoxia requires Notch signaling to maintain the undifferentiated cell state. *Dev Cell* 2005; **9**: 617–628.
46 Frid MG, Aldashev AA, Dempsey EC, Stenmark KR. Smooth muscle cells isolated from discrete compartments of the mature vascular media exhibit unique phenotypes and distinct growth capabilities. *Circ Res* 1997; **81**: 940–952.
47 Wohrley JD, Frid MG, Moiseeva EP, Orton EC, Belknap JK, Stenmark KR. Hypoxia selectively induces proliferation in a specific subpopulation of smooth muscle cells in the bovine neonatal pulmonary arterial media. *J Clin Invest* 1995; **96**: 273–281.
48 Morrow D, Scheller A, Birney YA, Sweeney C, Guha S, Cummins PM, Murphy R, Walls D, Redmond EM, Cahill PA. Notch-mediated CBF-1/RBP-J{kappa}-dependent regulation of human vascular smooth muscle cell phenotype *in vitro*. *Am J Physiol Cell Physiol* 2005; **289**: C1188–C1196.
49 Owens GK. Molecular control of vascular smooth muscle cell differentiation. *Acta Physiol Scand* 1998; **164**: 623–635.
50 Tang Y, Urs S, Liaw L. Hairy-related transcription factors inhibit Notch-induced smooth muscle alpha-actin expression by interfering with Notch intracellular domain/CBF-1 complex interaction with the CBF-1-binding site. *Circ Res* 2008; **102**: 661–668.
51 Kyriazis GA, Belal C, Madan M, Taylor DG, Wang J, Wei Z, Pattisapu JV, Chan SL. Stress-induced switch in Numb isoforms enhances Notch-dependent expression of subtype-specific transient receptor potential channel. *J Biol Chem* 2010; **285**: 6811–6825.
52 Lu W, Wang J, Peng G, Shimoda LA, Sylvester JT. Knockdown of stromal interaction molecule 1 attenuates store-operated Ca^{2+} entry and Ca^{2+} responses to acute hypoxia in pulmonary arterial smooth muscle. *Am J Physiol Lung Cell Mol Physiol* 2009; **297**: L17–L25.
53 Guo Q, Huang JA, Yamamura A, Yamamura H, Zimnicka AM, Fernandez R, Yuan JX. Inhibition of the $Ca^{(2+)}$-sensing receptor rescues pulmonary hypertension in rats and mice. *Hypertens Res* 2014; **37**: 116–124.
54 Lee HJ, Li N, Evans SM, Diaz MF, Wenzel PL. Biomechanical force in blood development: extrinsic physical cues drive pro-hematopoietic signaling. *Differentiation* 2013; **86**: 92–103.
55 Koutelou E, Sato S, Tomomori-Sato C, Florens L, Swanson SK, Washburn MP, Kokkinaki M, Conaway RC, Conaway JW, Moschonas NK. Neuralized-like 1 (Neurl1) targeted to the plasma membrane by N-myristoylation regulates the Notch ligand Jagged1. *J Biol Chem* 2008; **283**: 3846–3853.